Activity on *Leishmania tropica* of Metal Complexes with NNOO Tetradentate Schiff Base Ligand: Kinetic and Thermodynamic Studies from TG-DTA Analysis

[1]Muhammad Ikram*, [1]Sadia Rehman*, [2]Qaisar Jamal, [2]Akram Shah
[1]*Department of Chemistry, Abdul Wali Khan University Mardan, Pakistan.*
[2]*Department of Zoology, University of Peshawar, Peshawar 25120, Pakistan.*
ikram@awkum.edu.pk*

(Received on 5th November 2014, accepted in revised form 27th April 2015)

Summary: In the search for antileishmanial drug, tetradentate Schiff base ligand 2-{(E)-[(2-{[(Z)-(2-hydroxyphenyl)methylidene]amino}phenyl)imino]methyl}phenol (**H_2L**) was reacted with transition metal ions to yield the complexes of the composition ML [where M = Co (II), Ni (II), Cu (II), & Zn (II)]. The copper based compound **3** (IC_{50} = 5.857 µM) showed activities even higher than the standard drug. TG and DTA analyses under static air in the temperature range 30-1000 °C were also observed for all the compounds. The TG-DTA analyses and the subsequent themodynamic and kinetic parameters calculated using the TG-DTA curves, have potential relevance for the biological activities. Horowitz–Metzger method was applied for calculating the activation energies and order of pyrolysis. Thermodynamic parameters like ΔS*, ΔH* and ΔG* were subsequently calculated using the corresponding expressions. The order of decreasing thermal stability and decreasing activation energy follow the orders Ni(II) >Co(II)>Zn(II) >Cu(II) and $E^*_{Cu}>E^*_{Co}>E^*_{Ni}>E^*_{Zn}$, respectively.

Key Words: Schiff base, Leishmania, Coordination compounds, Trypanosoma tropica, Thermal studies, Kinetic and Thermodynamic studies

Introduction

Trypanosoma is a genus of kinetoplastids which is descendent of common ancestor, is a unicellular parasitic flagellate protozoa [1]. Trypanosome cause different human diseases like [1-5] African trypanosomiasis, South American trypanosomiasis and Leishmaniasis. Leishmaniasis is a set of trypanosomal diseases caused by various species of *Leishmanial* species. African trypanosomiasis is also known as sleeping Sickness whereas South American trypanosomiasis is known as chagas disease, both are caused by Trypanosoms. The former is caused by *Trypanosoma brucei* while the latter by *Trypanosoma cruzi*.

All trypanosomes are heteroxenous and complete their life cycles in more than one obligatory host. All trypanosomes are transmitted via a vector, majority of these vectors are belonging to blood-feeding invertebrates. The mechanism of transmission is also different among the different species [3]. Trypanosomatides occur in different morphological forms in its life cycle viz amastigote (leishmanial), promastigote (leptomonad), epimastigote (crithidial), trypomastigote (trypanosomal) and opisthomastigote (herpetomonad).

Leishmaniasis [5, 6] can be classified as:

- Visceral leishmaniasis is the most prevalent and serious form of the disease. It may find potential fatality if untreated and is standing second largest parasitic killer of the world. In this condition the patient feel fever, weight loss, mucosal ulcers, fatigue, anemia, and substantial swelling of the liver and spleen.
- Cutaneous leishmaniasis is the most common form of the disease, it leads to sore at the bite site which may heal taking a very long time but an unpleasant scar is left behind. This form of the disease may lead to any type of leishmaniasis if was not treated properly on time.
- Diffuse cutaneous leishmaniasis develops skin lesions like leprosy and is very difficult to treat.
- Mucocutaneous leishmaniasis is also called skin ulcers and spread from a simple scar tissue damage. It damages particularly the tissues of nose and mouth.

The visceral Leishmaniasis (fig 1) is the most fatal form of the disease. Cutaneous and muco-cutaneous form are, however, also very important for scaring and disfiguration of facial beauty leading to social stigmatization for females in particular. Status of cutaneous leishmaniasis has been declared by WHO as re-emerging in most of the endemic third world countries and is rapidly spreading into the developed countries through population expansion, military interventions and transcontinental traveling [7-10].

Fig. 1: Visceral Leishmaniasis.

*To whom all correspondence should be addressed.

Treatment

Antimony-containing drugs like meglumine antimoniate and sodium stibogluconate [9-15] are commonly used for the treatment of the leishmaniasis. Other drugs like amphotericin B, ketoconazole, miltefosine, paromomycin, pentamidine etc may also be used for the treatment. In case of cutaneous leishmaniasis surgery may be needed to correct the disfigurement and stigma caused by facial sores. Viral leishmaniasis is very hard to treat, the patients usually develop drug-resistant therefore their spleen has to be removed (splenectomy).

But these drugs may induce side effects like cardiotoxicity, hepatotoxicity, pancreatitis, anaphylactoid reaction, blood dyscrasias, dyspnea, facial edema, nephrotoxicity, anorexia, hypotension, nausea, vomiting, headache, tachypnea, drowsiness and many more [16-20]. Limited drug options, toxicity and development of parasite resistance to the current chemotherapeutic agents of the disease have created a dire need for searching new avenues both in the natural and synthetic pools. Therefore we synthesized the derivatives of essential metals for the treatment of leishmaniasis. The synthesized compounds were also studied for their thermal stabilities under static air. Schiff base ligands and their metal derivatives were used previously for many purposes including antimicrobial, enzyme inhibitory, anticancer, DNA binding, antiviral, etc [20-30]. Therefore, it was hypothesized that Schiff base derivatives may find use as antileishmanial candidate. The proposed application of the Schiff base metal derivatives is rarely studied. Our hypothesis proved to be valid as the metal derivatives were seen to be potential inhibitors of the leishmanial activity. Further detailed in vivo studies are needed to study the mechanism of action of the active compounds against leishmania.

Experimental

Materials and Methods

Analytical grade chemicals, buffers and solvents were used during the entire experimental manipulations. Solvents were purified and distilled at least twice before use. Chemical like metal(II) acetates (where metal(II) = Co, Ni, Cu and Zn) were obtained from Riedel-de-Haen. These metal salts were partially dehydrated by keeping in a vacuum oven for several hours set at 80 – 100^{o} C. 2,4-phenylenediamin was obtained from Sigma Aldrich and salicylaldehyde was obtained from Acros Organics.

Instrumentation

Elemental analyses were carried out on Varian Elementar II CHNS analyser. Atomic absorption spectrophotometer (Vario 6, Analytic Jena) operated on single beam mode was used for metal ion content in all samples. The concentration of each metal was determined against standard calibration curve with regression value (R2) of 0.9997 obtained with commercial standards (CPA Chem. Ltd Bulgaria). Melting points were recorded on a Gallenkamp apparatus. IR spectra were recorded using Shimadzo FTIR Spectrophotometer Prestige-21. ^{1}H-NMR were measured with Bruker DPX 400MHz (400.23 MHz) whereas, $^{13}C\{^{1}H\}$NMR were recorded on Bruker AV 400MHz (150.9 MHz) spectrometers in $CDCl_3$ at room temperature. Chemical shifts are reported in ppm and standardized by observing signals for residual protons. UV-Visible spectra were recorded on a BMS UV-1602. Molar conductance of the solutions of the metal complexes was determined with a conductivity meter type HI-8333. All measurements were carried out at room temperature with freshly prepared solutions. Magnetic susceptibilities were measured on a Sherwood Gouy Balance at room temperature calibrated with $Hg[Co(SCN)_4]$. Mass spectra were recorded on a LCT Orthogonal Acceleration TOF Electrospray mass spectrometer.

TG-DTA Analysis

The TG-DTA analyses were carried out using TG/DTA Diamond model by Perkin Elmer at heating rate 10 ^{o}C min^{-1} in temperature range 30-1000 ^{o}C under static air. Specific mass of samples were contained in ceramic pans crucibles adjusted on platform support giving a proportional signal to recorder, observed by computer interface and the results were plotted in the form of mass loss of sample vs. temperature for TG and microvolts vs. temperature for DTA. All the results were referenced to thermal decomposition of alumina. The activation energies of all the samples were calculated using Horowitz-Metzger method [31]. It was found that linear plots can be obtained while $\ln\ln (W_o - W_t^f)/(W - W_t^f)$ {where W_o = initial mass taken, W = weight remaining at a given temperature, W_t^f = final weight} were plotted against Θ {where $\Theta = T_c - T_s$}. The slope of the straight line was used to calculate the activation energy through the expression (1):

$$\text{Slope} = E^*/RT_s^2 \qquad (1)$$

Order of decomposition was calculated from the relationship between reaction order and concentration at maximum slope [31]. Thermodynamic parameters of activation were evaluated by using the following expressions (2), (3) and (4), respectively [32]:

$$\Delta S^* = 2.303\log[Ah/k_B T_s]R \quad (2)$$

$$\Delta H^* = \Delta E^* - RT \quad (3)$$

$$\Delta G^* = \Delta H^* - T\Delta S^* \quad (4)$$

Parasite Culture

Leishmania tropica KWH_{23} was cultured in 5 mL complete M199 medium at an initial parasite density of $1x10^6$. Growth was monitored for 10 days with every third day medium change after which the promatigotes reached to log or stationary phase where they stopped division and were ready for harvesting. Culture was maintained at a constant temperature of 26 ^{0}C.

Plating of Promastigotes and Drug Application

Promastigotes were plated in 96 well flat bottom plates at $1x10^5$/ well parasite density in complete M199 medium. Each compound was applied in three different concentration of 50µM, 16 µM and 4µM with quadruplicate for each concentration. Promastigotes were incubated with the compounds for 48 hours under the same temperature conditions as mentioned before. After 48 hours incubation with the test compounds, parasite density in each well was counted in an Improved Neubaur hemocytometer along with the negative control. Percent inhibition of the parasites caused by the compounds was calculated using the following formula:

% Inhibition= [Control –Treated/Control] × 100

The obtained data was processed in statistical software GraphPad Prism 6.01 to obtain the IC_{50} values for the compounds.

Synthesis of 2-{(E)-[(2-{[(E)-(2-hydroxyphenyl)methylidene]amino}phenyl)imino]methyl}phenol (H_2L)

Salicylaldehyde (1.2cm^3, 0.011mol) was added to a solution of 2,4-phenylenediamin (2.6g, 0.025mol) in ethanol which was stirred for 3hr. A yellow solution was obtained which turned to solid powder after sometime. The product was purified by washing with 10% copious n-hexane and methanol solution. (Yield: 1.5g, 85%). M.p. 190-191 ^{o}C. IR, : 3200(bd), 3053(w), 1610(s), 1585(s), 1558(s), 1479(s), 1448(w), 1400(w), 1361(s), 1274(s), 1190(s), 1149(s), 1114(s), 1043(s), 999(s), 975(s), 908(s), 854(s), 829(s), 786(s), 744(s), 640(s), 588(s) cm^{-1} . ^{1}H-NMR* (400.23 MHz, CD_3OD, 303k): δ = 11.0 (s, 1H, Ar-O<u>H</u>), 9.0 (s, 1H, -<u>H</u>C=N), 8.8 (s, 1H, H2), 8.10 (d, $^3J_{HH}$= 8.35Hz, 1H, H9), 8.0 (s,1H, H4), 7.8 (d, $^3J_{HH}$ = 7.72Hz, 1H, H6), 7.73(d, $^3J_{HH}$ = 7.9Hz, 1H, H8), 7.70(t, $^3J_{HH}$ = 7.55Hz,1H, H16), 7.4 (m, 1H, H17), 7.3 (d, $^3J_{HH}$ = 7.6, 1H, H18), 7.1(d, $^3J_{HH}$ = 8.03Hz, 1H, H15), 7.0 (d, $^3J_{HH}$ = 7.48Hz, 1H, H7) ppm, $^{13}C\{^1H\}$-NMR (150.9 MHz, CD_3OD, 303k), 165(H<u>C</u>=N-, C12), 162(Aromatic <u>C</u>-OH, C14), 147(C,C10), 146 (CH, C2), 142(C, C5), 134(CH, C15), 133(CH, C18), 129.4(CH, C17), 129.2 (CH, C16), 128(C, C3), 127.8 (CH, C6), 127.4 (CH, C7), 124.7(CH, C8), 116(CH, C9) ppm. Elemental Analysis ($C_{20}H_{16}N_2O_2$), Calc. C: 75.93%, H: 5.10%, N: 8.86%, Exp. C: 76.80%, H: 5.10%, N: 10.89%. EI-MS: *m/z* (%) 338.1253 (100%) $[C_{20}H_{16}N_2O_2+Na]^+$, Λ_m = 213 S/cm.

(* NMR assignment is according to scheme 1)

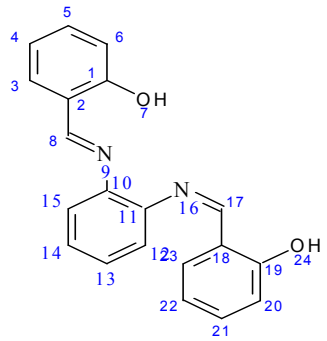

Scheme-1: Atoms numbering used for NMR signals.

Synthesis of [ML] where M=Ni, Co, Cu and Zn (II) acetates

0.011 mol of metal (II) acetates were stirred in a minimum volume of dried methanol and 0.020 mol of H_2L in a minimum volume of dried methanol was added to the metal solution. The mixture was stirred for 2-3 hrs at room temperature. The metal complex was collected after filtration and copiously washed several times with 5% n-hexane containing methanol.

Tetrakis(2-{(E)-[(2-{[(E)-(2-hydroxyphenyl) methylidene] amino}phenyl)imino] methyl} phenol)nickel(II) (1)

IR, : 1600(s), 1519(s), 1456(s), 1338(s), 1193(s), 1145(s), 1020(s), 929(s), 848(s), 752(s),

610(s), 535(s) cm^{-1} Elemental Analysis ($C_{20}H_{14}N_2NiO_2$), Calc. C: 64.40%, H:3.78%, N:7.51%, Ni:15.73%, Exp. C: 64.41%, H: 3.55%, N: 7.67%, Ni: 16.43%, MS: *m/z* (%)372.0403 (89%) $[C_{20}H_{14}N_2NiO_2]^+$ λ_{max} = 690nm (ε = 26 $M^{-1}cm^{-1}$, $^1A_{1g}\rightarrow{}^1A_{2g}$). μ_{eff}: 2.9B.M, Λ_m = 0.01 S/cm.

Tetrakis(2-{(E)-[(2-{[(E)-(2-hydroxyphenyl)methylidene]amino}phenyl)imino]methyl}phenol)cobalt(II) (2)

IR: 3010(w), 1604(s), 1573(s), 1519(s), 1456(s), 1375(s), 1336(s), 1244(s), 1186(s), 1145(s), 1126(s), 1043(w), 958(s), 920(s), 846(s), 802(s), 744(s), 617(s),583(s) cm^{-1} Elemental Analysis ($C_{20}H_{14}CoN_2O_2$), Calc. C: 64.35%, H: 3.78%, Co:15.79%, N:7.50%, Exp. C: 64.40%, H: 3.58%, N: 7.87%, Co: 15.67%, MS: *m/z* (%) 373.0381 (98%) $[C_{20}H_{14}CoN_2O_2]^+$, λ_{max}= 660nm (ε = 17 $M^{-1}cm^{-1}$, $^2A_{2g}\rightarrow{}^2B_{1g}$), μ_{eff}: 4.2 B.M. Λ_m = 0.01 S/cm.

Tetrakis(2-{(E)-[(2-{[(E)-(2-hydroxyphenyl)methylidene]amino}phenyl)imino]methyl}phenol)copper(II) (3)

IR: 1683(s), 1610(s), 1581(s), 1440(s), 1379(s), 1305(s), 1192(s), 1151(s), 1037(w), 927(s), 808(s), 752(s), 696(s), 558(s) cm^{-1} Elemental Analysis ($C_{20}H_{14}CuN_2O_2$), Calc. C: 63.57%, H:3.73%, Cu:16.82%, N:7.41%, Exp. C: 63.89%, H: 3.56%, N: 7.97%, Cu: 17.20%, MS: *m/z* (%) 377.0351 (100%) $[C_{20}H_{14}CuN_2O_2]^+$ λ_{max}= 810 nm (ε = 17.3$M^{-1}cm^{-1}$, $^2E\rightarrow{}^2T_2$). μ_{eff}: 1.5B.M. Λ_m = 0.01 S/cm.

Tetrakis(2-{(E)-[(2-{[(E)-(2-hydroxyphenyl)methylidene]amino}phenyl)imino]methyl}phenol)zinc(II) (4)

IR: 3010(w), 1612(s), 1525(s), 1456(s), 1384(s), 1323(s), 1244(s), 1174(s), 1151(s), 1126(s), 1029(s), 918(s), 854(s), 746(s) cm^{-1} Elemental Analysis ($C_{20}H_{14}N_2O_2Zn$), Calc. C: 63.26%, H:3.72%, N:7.38%, Zn:17.22%, Exp. C: 63.44%, H: 3.50%, N: 7.37%, Zn: 17.20%, MS: *m/z* (%) 378.0341 (100%) $[C_{20}H_{14}N_2O_2Zn]^+$, Λ_m = 0.01 S/cm.

Results and Discussion

Spectral studies of Schiff base ligand (H_2L) and its transition metal complexes

Schiff base ligand was synthesized by condensing salicylaldehyde and 1,2-phenylenediammine in equimolar ratio. The ligand **H_2L** was fully characterized by various analytical and spectroscopic techniques including elemental analyses, conductance studies, ^{1}H-NMR, $^{13}C\{^1H\}$-NMR, ES^+-MS and IR analysis. Elemental analytical data and ES^+-MS reveal the composition of the ligand and the metal complexes. Infrared spectra were observed in the region of 4000-400 cm^{-1} which shows a broad peak around 3400cm^{-1} for **H_2L**. This peak was assigned to the vibrational motion of aromatic hydroxyl group. A peak around 2800cm^{-1} is assigned to the zwitterionic linkage produced by hydrogen bond formation in HC=N- group. The vibration for Schiff base linkage is observed around 1585cm^{-1} showing the formation of the **H_2L** ligand. The Schiff base ligand is acting as quadridentate dianionic chelating agent and produces symmetric square planar complexes with metal ions like Co (II), Ni (II), Cu (II), and Zn (II). All the complexes were also characterized by analytical and spectroscopic methods of study. The elemental analytical data was found to be conforming to the composition where a ligand is attacking the metal center through four sites of attachment and produce symmetric metal complexes. The composition of the metal complexes was also confirmed by the high resolution ES^+-MS. The ligand was found to be acting as quadridentate dianionic ligand. The dianionic nature of the ligand was confirmed by the disappearance of vibrational band for hydroxyl group. The Schiff base linkage was also observed to be shifted by $\Delta\upsilon$ = 15-20cm^{-1} upon complexation with the metal ions.. The dianionic nature of the ligand was confirmed by the molar conductance values of the **H_2L** ligand (Λ_m = 213 S/cm). It is confirmed that all the metal complexes are non-electrolyte in nature.

The UV-visible spectra of the metal complexes **1**, **2**, and **3** were measured in the region of 200-1000 nm. Spectra for all the compounds were found to be showing only one absorption band each. A major absorption band around 690 nm was observed for **1** which was assigned to a transition $^1A_1g\rightarrow{}^1A_2g$. For a square planar geometry other charge transfer bands like $^1A_1g\rightarrow{}^1B_1g$ and $^1A_1g\rightarrow Eg$ are expected to be observed in the lower absorption region. However, such absorption bands may be observed in purified samples, but for the other compounds all the said bands are buried beneath the absorption region for $^1A_1g\rightarrow{}^1A_2g$ [21]. The crystal field splitting between the two sets of dyz, dzx and dz^2 orbitals and dxy and dx^2-y^2 orbitals is large. Furthermore, the energies between the dxy and dx^2-y^2 orbitals calculated from visible spectrum (ΔE = 1.79x10^{-3}ev) show closeness between the two orbitals allowing the occupation of single electron each. This behavior also explains the calculated magnetic susceptibility 2.9 B.M $\mu_{effective}$ value [22]. The splitting of orbitals is shown in fig.2.

Ligand-to-metal transitions in nickel square planar complexes were studied exclusively by Gray and Ballhausen [21]. It was unambiguously observed

that the two charge-transfer bands discussed above in complexes without an intraligand π system, are separated by nearly 10,000 cm^{-1}. Whereas in contrast situation metal-to-ligand charge-transfer transitions are more closely spaced. Herein the approximate separation between each band is 2000-3000 cm^{-1} [21,22]. The metal complexes formed with the aromatic dianionic ligand **H_2L** are therefore expected to yield transitions which will overlap in a narrow range and the other charge transfer bands are buried within the only major absorption observed.

The absorption for **2** occur at 660 nm (ε = 17 $M^{-1}cm^{-1}$) was tentatively assigned to the $^2A_{2g}\rightarrow{}^2B_{1g}$ transition. Cobalt complex while in C_{2v} symmetry show absorption for the transitions $^2A_{2g}\rightarrow{}^2B_{1g}$ and $^2A_2\rightarrow{}^2A_1$ where the former is allowed and the latter forbidden. The 4.0 B.M $\mu_{effective}$ value and the visible absorption band for **2** show the formation of two set of orbitals i.e. dyz and dzx set of orbitals and the dz^2, dxy, dx^2-y^2 set of orbitals (closely spaced). The crystal filed splitting ($\Delta E = 1.87 \times 10^{-3}$ev) between dz^2 and the dxy, dx^2-y^2 set of orbitals is not very high as compared to complex **1** (Fig. 2). Therefore it was presumed that each of dz^2 and dxy orbitals are occupying a single electron resulting in a high spin cobalt complex. For **3** the visible band observed at 810 nm is assigned to the $^2E\rightarrow{}^2T_2$ distorted square planar transition.

These charge transfer transitions are actually arising from the transition of pπ electrons residing the phenolate ion to dπ* metal orbitals. The pπ electrons residing on nitrogen of -C=N are also donated to the dπ* orbital of the metal ion which lead to transitions occurring in the region of 500-700 nm. However, these bands are weak enough to be obscured by the more intense phenolate to metal ion transitions [22].

Thermodynamics and Thermal studies

The Schiff base ligand and its metal complexes were also studied for their thermal degradation in the range of 30-1000 ^oC under static air. The TG and DTA curves are shown in figure 3 and 4, respectively whereas the respective data of the thermal degradation process is shown in Table-1. The endothermic peaks exhibited by all the compounds correspond to melting points and transition temperatures. The temperature at which a compound starts its decomposition is represented by T_d in table 1.The TG curve for **H_2L** shows that the compound is stable up to 225 ^oC and then follows the degradation process. T_d for **1, 2, 3** and **4** are 396, 332, 139 and 180 ^oC respectively. The thermodynamic and kinetic parameters are enlisted in table 2.

Table-1 enlists the data for degradation moieties and the DTA analytical data. It shows that the ligand exhibit five DTA peaks marking the five products of pyrolysis. The very large negative value for entropy, shown in table 2, explains the stable nature of the ligand, also confirmed by other thermodynamic factors. **H_2L** follows two step degradation (Scheme-2), producing the quinaxaline, hydrogen peroxide, and one mole hydrogen in the first step followed by degradation of the remaining moiety to biphenylene. No residue left at the end of the whole process of degradation. The degradation process completes at 760 ^oC. It was also presumed that hydrogen peroxide diproportionates to water and oxygen molecule.

$C_{20}H_{16}N_2O_2 \rightarrow C_8H_6N_2 + H_2O_2 + H_2 + C_{12}H_8^*$ I Stage
$C_{12}H_8^* \rightarrow C_{12}H_8$ II Stage

Scheme-2: Thermal degradation of H_2L.

All the transition metal complexes show same structure whereby the metal ion is surrounded by a single tetradentate ligand producing square planar geometry. But after looking into table 2 it was revealed that some major factor is operating in the stabilities of these compounds. The negative activation energies of all the transition metal complexes points toward Lindmann mechanism of degradation where other complex processes are also assigned apart from the simple degradation. Nickel based metal (II) complex **1,** exhibited the degradation to quinaxaline in the first stage like **H_2L**, with four marked DTA peaks. It was assigned that actually two diradical species are produced such as benzene diradical and ethanedinitrile diradical (Scheme-3). Both of these diradicals fuse together to produce quinaxaline product. In the second stage of degradation three moieties like biphenylene, water and one mole dioxygen are released with only one endothermic DTA peak. It was observed that the third and last stage is comprised of reduction of nickel oxide into neutral nickel. The negative entropy value points to the forward mechanism where 3/2 order is followed. The high enthalpy of activation and high Gibb's free energy of activation reveal the stable nature of the compound. The negative activation energy marks the complex mechanism of degradation.

$C_{20}H_{14}N_2NiO_2 \rightarrow C_8H_6N_2 + C_{12}H_8NiO_2$ I Stage
$C_{12}H_8NiO_2 \rightarrow C_{12}H_8 + H_2O + 1/2O_2 + NiO$ II Stage
$NiO \rightarrow Ni(Residue) + 1/2O_2$ III Stage

Scheme-3: Thermal degradation of **1**

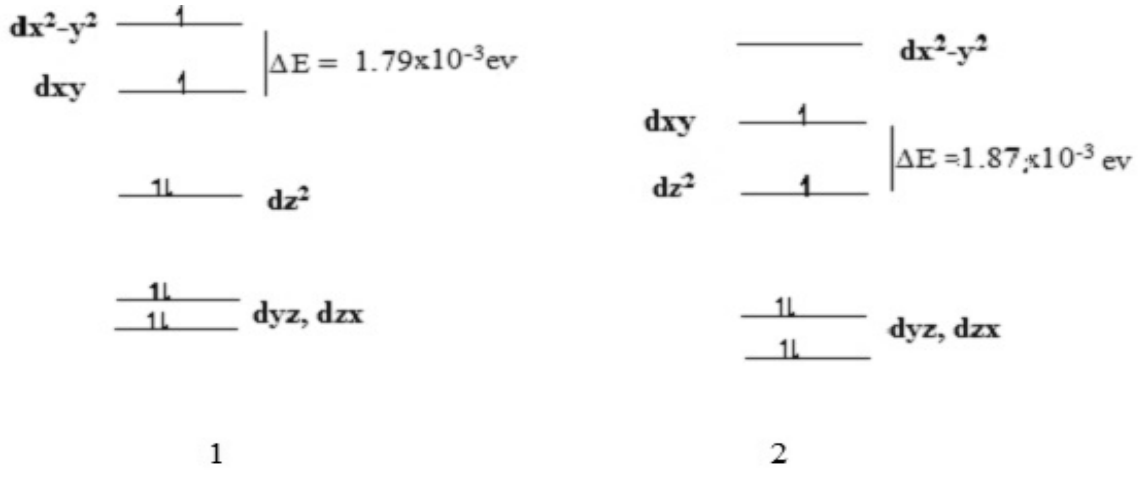

Fig. 2: Crystal field splitting for 1 and 2 on the basis of UV-Visible and $\mu_{effective}$.

Table-1: Thermoanalytical results of H_2L and its complexes.

Compound	TG Temp. range/ °C	Decomposition Temperature/ oC	Stage	Mass loss		DTA	Moiety evolved
				% Calc.	% Found		
H_2L	30-460	225	I	51.8	50.5	5.98, (-)9.58, (-)13.57	H_2O_2, $C_8H_6N_2$
	> 460		II	48.1	49.2	(-)10, (+)19.53	$C_{12}H_8$
1	30-461	396	I	34.8	31.8	(+) 2.84, (-)25.81, (-)14.48, (-)9.08	$C_8H_6N_2$(in crystal lattice)
	461-563		II	50.0	51.1	(+)107.52	$C_{12}H_8$, H_2O, $1/2O_2$
	>563		Res	15.7	16.1	---	Ni
2	30-377	332	I	10.9	10.8	(-)13.23, (+)2.99, (-) 10.88, (-)14.95	C_2H_2, $1/2N_2$
	377-535		II	73.3	73.9	(+)86.35	$C_{18}H_{16}O_3$
	>535		Res	15.7	15.7	---	Co
3	30-321	139	I	26.1	26.9	(+)1.9, (-)4.2, (-)4.98, (+) 3.92	$C_6H_4O_2$
	321-630		II	60.0	62.9	(+)34.22, (+) 21.21	$C_{12}H_{10}O_2$, $(CN)_2$
	>630		Res	16.8	14.2	---	Cu
4	30-240	180	I	7.3	7.1	(-)2.61, (-)14.21	C_2H_4
	240-585		II	75.3	76.3	(-)19.32, (+)68.55	$C_{12}H_6O_2$, $C_6H_4N_2$
	>585		Res	20.0	21.4	---	ZnO

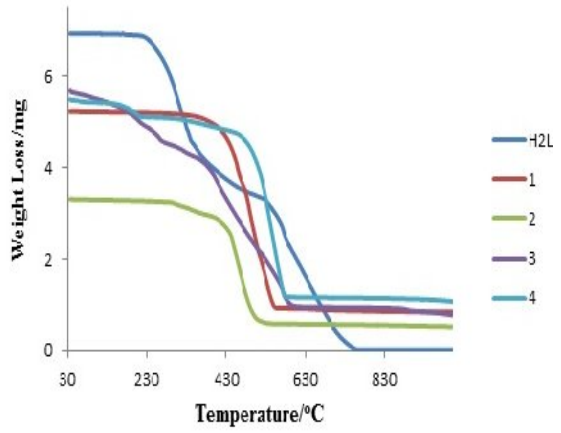

Fig. 3: Thermogravimetric plots of H_2L and its metal complexes.

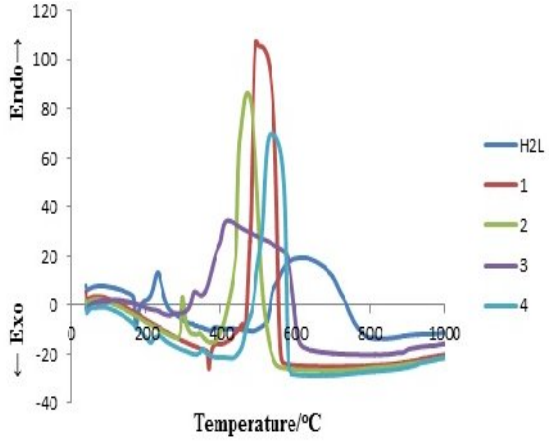

Fig. 4: Differential thermogravimetric curves for H_2L and its metal complexes. °C.

The compound **2**, exhibits three stage degradation which starts around 330 ^{o}C. In the first stage unlikely to compound **1**, four DTA peaks represent the formation of two marked products viz dinitrogen and ethene gas. All the peaks are exothermic except the peak at 2.99 which explains its apparent relationship with dinitrogen gas formation (Scheme-4). The second stage of degradation marked by a huge endothermic peak show the formation of a single product which was calculated to be 6,6-bis(2-hydroxyphenyl)hexa-2,4-diynal formed by several intermediate reactions. The final stage, like compound **1,** is following the release of oxygen gas leaving behind cobalt metallic residue. The negative entropy value suggests the stable nature of the complex. The degradative process was observed to be following 5th order kinetics. Strangely negative value for enthalpy of activation was observed suggesting the exergonic nature of the complex. The Gibb's free energy of activation has positive value showing the stable quadridentate nature of ligand surrounding the metal center. Similar explanation like **1** may be assigned to the negative activation energy of compound **2**.

$C_{20}H_{14}CoN_2O_2 \rightarrow C_2H_2 + 1/2N_2 + C_{18}H_{12}CoO_2$ I Stage
$C_{18}H_{12}CoO_2 \rightarrow C_{18}H_{12}O_3 + CoO$ II Stage
$CoO \rightarrow 1/2O_2 + Co$(Residue) III Stage

Scheme-4: Thermal degradation of **2**

Compound **3** demonstrates two stages of thermal degradation leaving behind copper as residue. The degradative process starts around 139 ^{o}C and goes beyond 630 ^{o}C encompassing many intermediate stages. At the first stage of thermal degradation, it was calculated that hex-2-en-4-ynedial is produced by the degradation of benzene ring (scheme 5). The second stage of degradation starts around 320 ^{o}C. This stage is marked by two endothermic peaks. Cyanogen gas is presumed to be produced in very small amount. The other moiety released may be biphenol like 2-[(E)-(quinolin-3-ylimino)methyl]phenol reported previously [29, 30]. Beyond 630 ^{o}C, copper (II) is presumed to be reduced to metallic copper by some catalytic process. This compound also show negative entropy of activation, negative enthalpy of activation, positive Gibb's free energy of activation and negative activation energy with 5th order kinetics for the whole degradative process. Therefore same explanation may be assigned as in previous case.

$C_{20}H_{14}CuN_2O_2 \rightarrow C_6H_4O_2 + C_{14}H_{10}CuN_2O_2$ I Stage
$C_{14}H_{10}CuN_2O_2 \rightarrow C_{12}H_{10}O_2 + (CN)_2 + CuO$ II Stage
$CuO \rightarrow 1/2O_2 + Cu$ (Residue) III Stage

Scheme-5: Thermal degradation of 3

The compound **4** is thermally cleaved around 180 ^{o}C. The first stage of degradative process reveals the formation of ethene with two exothermic DTA peaks. After the completion of first stage of degradataion around 240 ^{o}C, the second stage starts where one endothermic and one exothermic peak are observed. One of the product produced in this stage is assigned to be (4*E*,8*E*)-dodeca-4,8-diene-2,6,10-triynedial and the other one is hexa-2,4-dinitrile. Zinc oxide remains as residue beyond 580 ^{o}C. Compounds **3** and **4** behave exactly the same for their thermodynamic and kinetic parameters.

$C_{20}H_{14}N_2O_2Zn \rightarrow C_2H_4 + C_{18}H_{10}N_2O_2Zn$ I Stage
$C_{18}H_{10}N_2O_2Zn \rightarrow C_{12}H_6O_2 + C_6H_4N_2 + ZnO$ (Residue) II Stage

Scheme-6: Thermal degradation of **4**

From the T_d values of all complexes it can be established that Ni(II) complexes are stable. The order of stability varies viz; Ni(II) >Co(II)>Zn(II) >Cu(II) which follow the Irving William series of stabilities. From the activation energies the order of decreasing activation energy is $E^*_{Cu} > E^*_{Co} > E^*_{Ni} > E^*_{Zn}$.

Biological Evaluation: Frequency of Leishmaniasis in Pakistan, A survey

The prevalence of both visceral and mucocutaneous Leishmaniasis in various parts of KPK Pakistan, particularly in border areas and southern region was violent. This necessitated survey work was conducted in the area of Khyber agency in order to explore Leishmanial parasites in representative areas like main central city, in the entire year. The survey showed highest patient frequency in the April and October months which increased continuously and were adopting endemic. The frequency of the patients was found minimum in the month of November.

Result can clearly be interpreted from the Table-3 and it become obvious from the data listed that the disease frequency is extremely high in the month of april, 2012 in which the infected patients were eighty one (81) followed by May, 2012 with thirty two (32) patients.

In the same table the months of September and November 2012 showed minimum numbers (Six) of infected patients followed by July in which the infected patients were eight. In the rest of the results if we notice the table it is found that the infected patients ratio is between ten (10) to twenty five (25).

Table-2: Kinetic and thermodynamic parameters of H-QMP and its metal complexes.

Compound	Ts in K	E*, KJ/mol	ΔH*, KJ/mol	ΔG^*, KJ/mol	ΔS^*, $Jmol^{-1}K^{-1}$	Order of reaction, n
H_2L	595	8.83	3.88	151.55	-248.11	∞
1	767.7	-47.04	53.42	141.82	-254.30	3/2
2	737	-37.03	-43.15	157.01	-271.77	5
3	671.5	-20.99	-26.57	145.18	-255.77	5
4	787.2	-47.91	-54.45	154.33	-265.33	5

If we campare the data of January, February, 2012 and January, February 2013 we can see almost same ratio of the infected patient. So from the results it can be concluded the particular month of the year have key role in the spread of the disease in Khyber agency region.

Table-3: Number of patients suffering from Leishmaniasis.

S.No	Report collection date	Numbers of Patients
1	January, 01, 2012	14
2	February, 01, 2012	25
3	March, 01, 2012	27
4	April, 01, 2012	81
5	May, 01, 2012	32
6	June, 01, 2012	21
7	July, 01, 2012	08
8	August, 01, 2012	11
9	September, 01, 2012	06
10	October, 01, 2012	19
11	November, 01, 2012	06
12	December, 01, 2012	17
13	January, 01, 2013	10
14	February, 01, 2013	21

In vitro antitrypanosomal activity

Leishmaniasis, an emerging and uncontrolled category I disease is adopting alarming conditions in Khyber agency of KPK Pakistan. The current antimonial drugs used for the treatment of leishmaniasis are not totally safe and active because of increasing variation and adaptibilty in the microbes. Therefore, the Schiff base ligand and its transition metal compounds were tested In vitro for their antileishmanial activities using *Leishmania tropica* KWH_{23}. The results were compared with standard drugs reported earlier [23-26]. All the compounds show variation in degree of antileishmanial activities against promastigotes of *L. tropica* KWH_{23}. Table-4 Show that the parent quadridentate Schiff base ligand **H_2L** showed IC_{50} value of 52.56 µM. in comparison to the metal derivatives of the same ligand which showed very good results. Compound **1**, **2**, **3**, and **4** show 36 µM, 13.59 µM, 5.85 µM and 26.59 µM inhibition. Compound **3** show comparable result and is found the most active compound of all. Its activity is even higher than the standard drug nifurtimox reported earlier. Compound **3** is even comparable to all the compounds in its % inhibition at different concentrations such as at 4 µM it shows 79 % inhibition (fig 5). The high activity of copper based compound **3** is also comparable to its antimicrobial activity [27]. The activities of all the compounds may be assigned to the presence of transition metal ions which impart geometric restrains and electronic effects. The new geometry also may also enhance the lipophilicity of the compounds in cell matrix [19]. The neat ligand is found to be very less lipophilic which ultimately cause reduction in its activity. It was observed that the presence of metal ion enhances the antileishmanial activities because of the possible catalytic interaction of metal center with DNA of leishmania. It was suggested that the interaction of metal compounds with DNA of promistigote through intercalative mode, cause damage to the DNA [28].

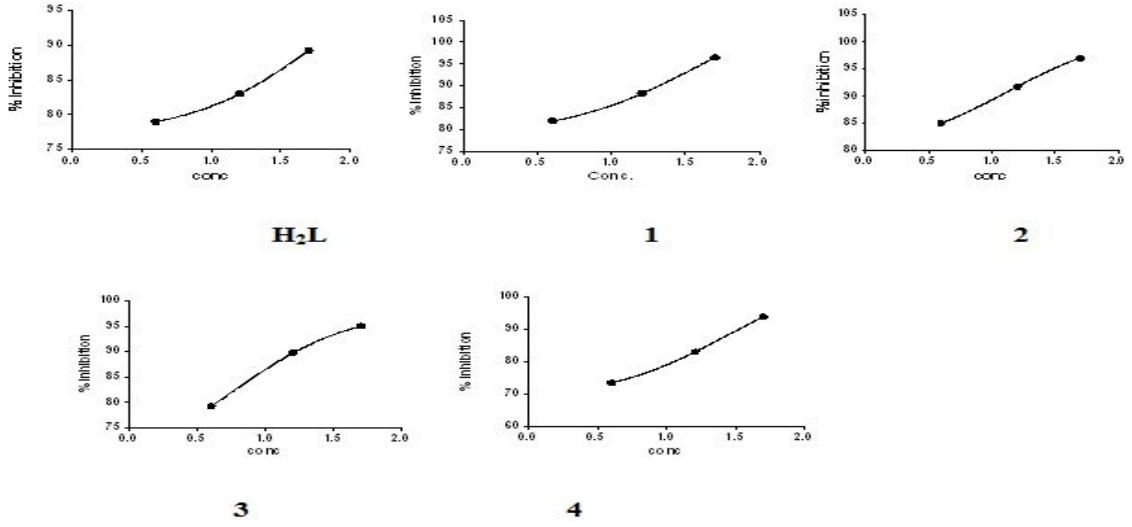

Fig. 5: Percent inhibition of Leishmania at 4 µM, 16 µM and 50 µM concentrations.

Table-4: *In vitro* antileishmanail evaluation of H_2L and its transition metal (II) complexes.

Compound	% Inhibition for 50µM	% Inhibition for 16µM	% Inhibition for 4µM	IC_{50} (µM)
H_2L	89	83	79	52.56
1	96	88	82	36
2	97	91	85	13.59
3	95	89	79	5.85
4	93	83	73	26.59
Nifurtimox	---	---	---	7.70
Amphotericin B	---	---	---	0.15

Conclusions

Tetradentate NNOO type ligand 2-{(E)-[(2-{[(Z)-(2-hydroxyphenyl) methylidene] amino} phenyl) imino] methyl}phenol (**H_2L**) was reacted with Co (II), Ni (II), Cu (II) and Zn (II) metal ions to produce geometrically rigid square planar compounds. All the synthesized compounds were studied for their antileishmanial activities against *Leishmania tropica* KWH_{23} and it was found that metal complexation make the Schiff base ligand much more active than the neat ligand by reorientation and electronic effects. By comparing the IC_{50} values it was observed that copper based Schiff base metal complex was more active than the tested compounds and even the standard compound Nifurtimox. In this paper we have shown that the easily accessible tetradentate ligand $\mathbf{L}^{2-}$ in combination with transition metal ions in general and with Copper in particular can be used to treat visceral or related leishmaniasis. The compounds were hypothesized that greater the stability of compounds greater will be the activity. By comparing the activation energies of degradation it was concluded that the order of decreasing activation energies is $E^*_{Cu}>E^*_{Co}>E^*_{Ni}>E^*_{Zn}$. Therefore by comparison of the IC_{50} values it was seen that the order of increasing IC_{50} values is IC_{50}-CuL>IC_{50}-CoL>IC_{50}-ZnL>IC_{50}-NiL>>IC_{50}-H_2L. The inhibitory studies and thermal stabilities can be correlated with each other up to a great extent. Hence it may be concluded that copper based transition metal complex deserves further developments and may be tested for In vivo studies at other trypanosome stage as well.

Acknowledgment

The authors are gratefully acknowledged to the Higher Education Commission (HEC) Pakistan for providing financial assistance.

References

1. M. P. Barrett, S. L. Croft, Management of Trypanosomiasis and Leishmaniasis, *Br. Med. Bull.,* **104**: 175 (2012).
2. W. D. James, T. Berger and D. Elston, *Andrews' Diseases of the Skin, Clinical Dermatology*. Saunders Elsevier. pp. 422. (2006).
3. K. Aoun, A. Bouratbine, Cutaneous Leishmaniasis in North Africa: a review, *Parasite*, **21**, 14 (2014).
4. M. P. Accioly, C. M. L. Bevilaqua, F. C. M. Rondon, S. M. de Morais, L. K. A. Machado, C. A. Almeida, H. F. de Andrade Jr., R. P. A. Cardoso, Leishmanicidal Activity in Vitro of Musa Paradisiaca L. and *Spondias mombin L.* fractions, *Vet. Parasitol.,* **187**, 79 (2012).
5. S. Sundar, J. Chakravarty, Leishmaniasis: an Update of Current Pharmacotherapy, *Exper. Opinion Pharmacother.* **14**, 53 (2013).
6. P. Minodier and P. Parola, Cutaneous Leishmaniasis Treatment, *Travel Med. Infect. Dis.,* **5**, 150 (2007).
7. A. Pavli and H. C. Maltezou, Leishmaniasis, an Emerging Infection in Travelers, *Int. J. Infect. Dis*., **14**: 1032 (2010).
8. R. Nagill and S. Kaur, Vaccine Candidates for Leishmaniasis: A Review. *Int. Immunopharmacol.,* **11**, 1468 (2011).
9. L. H. Freitas-Junior, E. Chatelain, H. A. Kim and J. L. Siqueira-Neto, Visceral Leishmaniasis Treatment: What Do We Have, What Do We Need and How to Deliver It? *Int. J. Parasitol. Drugs Drug Resist.,* **2**: 11 (2012).
10. B. Purkait, A. Kumar, N. Nandi, A. H. Sardar, S. Das, S. Kumar, K. Pandey, V. Ravidas, M. Kumar, T. De, D. Singh and P. Das, Mechanism of Amphotericin B Resistance in Clinical Isolates of Leishmania donovani, *Antimicrob. Agents Chemother.,* **56** , 1031 (2012).
11. S. A. Ejazi, N. Ali, Developments in Diagnosis and Treatment of Visceral Leishmaniasis During the Last Decade and Future Prospects.". *Expert Rev. Anti Infect. Ther.* **11**, 79 (2013).
12. T. P. Dorlo, M. Balasegaram, J. H. Beijnen, P. J. de Vries, Miltefosine: a Review of its Pharmacology and Therapeutic Efficacy in the Treatment of Leishmaniasis", *J. Antimicrobial. Chemotherapy,* **67**, 2576 (2012).
13. K. M. Ahua, J. Ioset, K. N. Ioset, D. Diallo, J. Mauël and K. Hostettmann, Antileishmanial Activities Associated with Plants Used in the Malian Traditional Medicine, *J. Ethnopharmacol.,* **110**: 99 (2007).
14. V. S. Amato, F. F. Tuon, H. A. Bacha, V. A. Neto and A. C. Nicodemo, Mucosal Leishmaniasis Current Scenario and Prospects for Treatment, *Acta Trop.,* **105**: 1 (2008).
15. S. B. Bharate, J. B. Bharate, S. I. Khan, B. L. Tekwani, M. R. Jacob, R. Mudududdla, R.

Yadav, R. B. Singh, P. R. Sharma, S. Maity, B. Singh, I. A. Khan and R. A. Vishwakarma, Discovery of 3,30-diindolylmethanes as potent antileishmanial agents, *Eur. J. Med. Chem.,* **63**: 435 (2013).
16. L. F. Oliveira, A. O. Schubach, M. M. Martins, S. L. Passos, R. V. Oliveira, M. C. Marzochi, and C. A. Andrade, Systematic Review of the Adverse Effects of Cutaneous Leishmaniasis Treatment in the New World. *Acta Trop*., **118**, 87 (2011).
17. F. Poorrajab, S. K. Ardestani, S. Emami, M. Behrouzi-Fardmoghadam, A. Shafiee and A. Foroumadi, Nitroimidazolyl-1,3,4-thiadiazole-based anti-leishmanial agents: Synthesis and in Vitro Biological Evaluation. *Eur. J. Med. Chem.* **44**, 1758. (2009).
18. C. Marín, M. P. Clares, I. Ramírez-Macías, S. Blasco, F. Olmo, C. Soriano, B. Verdejo, M. J. Rosales, D. Gomez-Herrera, E. García-España and M. Sánchez-Moreno, In Vitro Activity of Scorpiand-Like Azamacrocycle Derivatives in Promastigotes and Intracellular Amastigotes of Leishmania Infantum and Leishmania Braziliensis. *Eur. J. Med. Chem.,* **62**, 466 (2013).
19. D. Santos, B. Parajón-Costa, M. Rossi, F. Caruso, D. Benítez, J. Varela, H. Cerecetto, M. González, N. Gómez, M. E. Caputto, A. G. Moglioni, G. Y. Moltrasio, L. M. Finkielsztein, D. Gambino, Activity on Trypanosoma Cruzi, Erythrocytes Lysis and Biologically Relevant Physicochemical Properties of Pd(II) and Pt(II) Complexes of Thiosemicarbazones Derived from 1-indanones, *J. Inorg. Biochem.* **117**, 270 (2012).
20. I. Machado, M. Fernández, L. Becco, B. Garat, R. F. Brissos, N. Zabarska, P. Gamez, F. Marques, I. Correia, J. C. Pessoa, D. Gambino, New Metal Complexes of NNO Tridentate Ligands: Effect of Metal Center and co-ligand on Biological Activity, *Inorg. Chim. Acta,* **420**, 39 (2014).
21. H. B. Gray, C. J. Ballhausen, A Molecular Orbital Theory for Square-Planar Metal Complexes, *J. Am. Chem. Soc.* **85**, 260 (1963).
22. M. Ikram, S. U. Rehman, S. Rehman, R. J. Baker, C. Schulzke, Synthesis, Characterization and Distinct Butyrylcholinesterase Activities of Transition Metal [Co(II), Ni(II), Cu(II) and Zn(II)] complexes of 2-[(E)-(quinolin-3-ylimino)methyl]phenol, *Inorg. Chim. Acta,* **390**, 210 (2012).
23. A. Merlino, D. Benitez, S. Chavez, J. Da Cunha, P. Hernández, L. W. Tinoco, N. E. Campillo, J. A. Páez, H. Cerecetto, M. González, Development of Second Generation Amidinohydrazones, Thio- and Semicarbazones as *Trypanosoma cruzi* inhibitors bearing benzofuroxan and benzimidazole 1,3-dioxidecore scaffolds, *Med. Chem. Comm.* **1**, 216. (2010).
24. M. E. Caputto, L. E. Fabian, A. G. Moglioni, G. Y. Moltrasio, D. Benítez, A. Merlino, H. Cerecetto, M. González, L. M. Finkielsztein, *Bioorg. Med. Chem.* **19**, 6818. (2011).
25. M. Ikram, S. Rehman, A. Khan, R. J. Baker, T. S. Hofer, F. Subhan, M. Qayum, Faridoon, C. Schulzke, Synthesis, Characterization, Antioxidant and Selective Xanthine Oxidase Inhibitory Studies of Transition Metal Complexes of Novel Amino Acid Bearing Schiff Base Ligand, *Inorg. Chim. Acta,* article in press, (2015).
26. M. Navarro, Gold Complexes as Potential Anti-Parasitic Agents, *Coord. Chem. Rev.* **253**, 1619 (2009).
27. M. Ikram, S. Rehmanm Faridoon, R. J. Baker, H. U. Rehman, A. Khan, M. I. Choudhary and S. U. Rehman, Synthesis, and Distinct Urease Enzyme Inhibitory Activities of Metal Complexes of Schiff-Base Ligands: Kinetic and Thermodynamic Parameters Evaluation from TG DTA Analysis, *Thermochim. acta,* **555**, 72 (2013).
28. M. Ikram, S. Rehman, M. Ali, Faridoon, C. Schulzke, R. J. Baker, A. J. Blake, K. Malook, H. Wong and S.-U. Rehman, Urease and α-chymotrypsin Inhibitory Activities of Transition Metal Complexes of New Schiff Base Ligand: Kinetic and Thermodynamic Studies of the Synthesized Complexes Using TG DTA Pyrolysis, *Thermochim. acta,* **562C**, 22 (2013).
29. S. A. Patil , C. T. Prabhakara, B. M. Halasangi, S. S. Toragalmath, P. S. Badami, DNA Cleavage, Antibacterial, Antifungal and Anthelmintic Studies of Co(II), Ni(II) and Cu(II) Complexes of Coumarin Schiff Bases: Synthesis and Spectral Approach, *Spectrochim. Acta Mol. Biomol. Spectros.,* **137**, 641, (2015).
30. S. P. Kumar, R. Suresh, K. Giribabu, R. Manigandan, S. Munusamy, S. Muthamizh, V. Narayanan, Synthesis and Characterization of Chromium(III) Schiff Base Complexes: Antimicrobial Activity and its Electrocatalytic Sensing Ability of catechol, *Spectrochim. Acta Mol. Biomol. Spectros.,* **139**, 431 (2015).
31. H. H. Horowitz and G. Metzger, A New Analysis of Thermogravimetric Traces, *Anal. Chem.* **35**, 1464 (1963).
32. M. Olszak-Humienik, J. Mozejko, Thermodynamic Functions of Activated Complexes Created in Thermal Decomposition Processes of Sulphates, *Thermochim. Acta*, 344, 73. (2000).